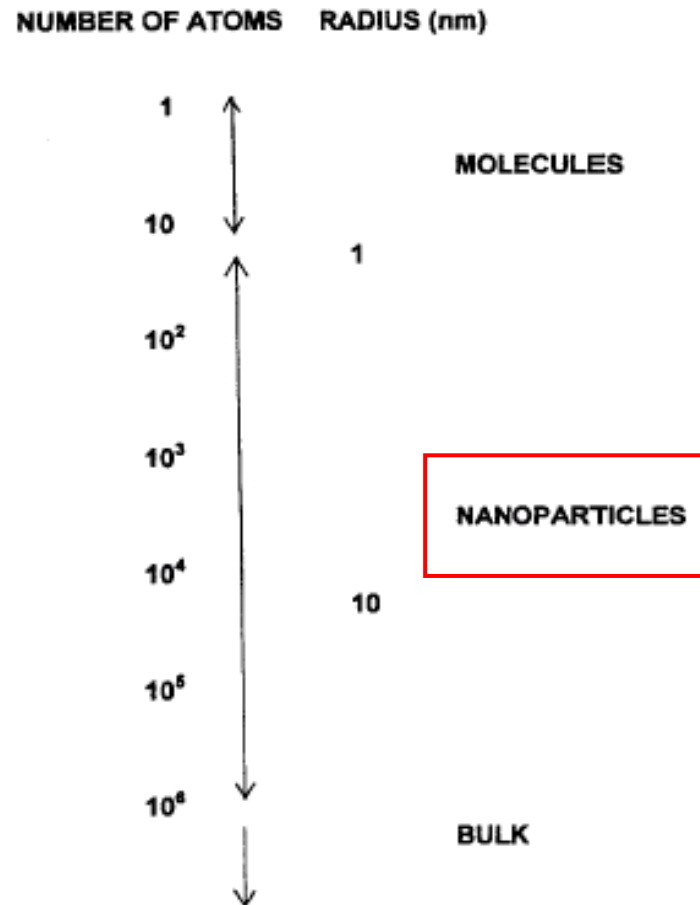
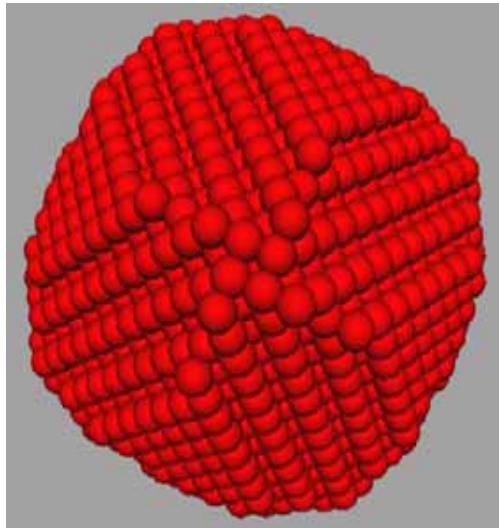


Properties of individual nanoparticles



Au nanoparticle as an example



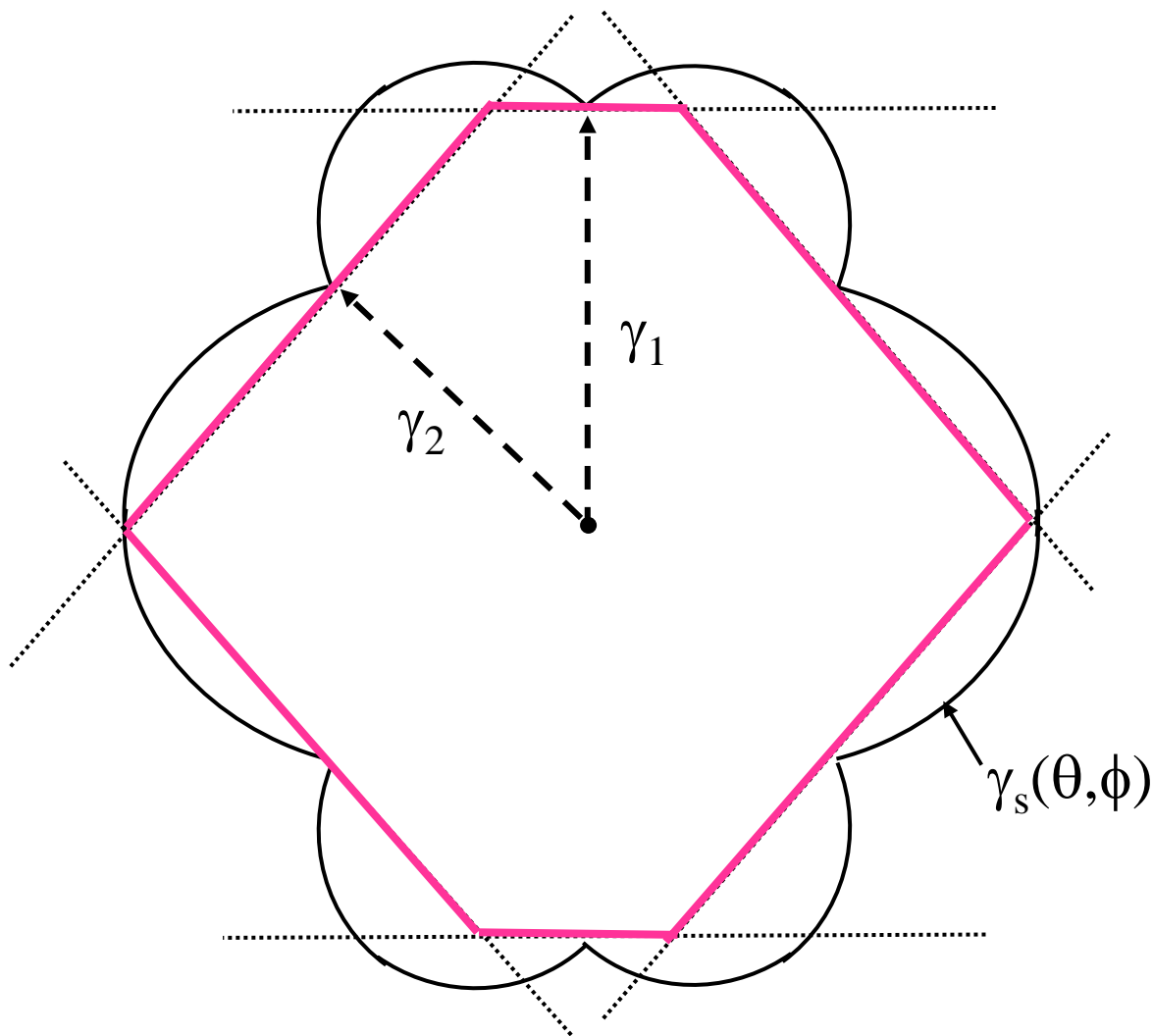
← 10 nm →

Number of valence electrons (N) contained in the particles is roughly 40,000. Assume the Fermi energy (E_F) is about 7 eV for Au, then

$$E_F/N \sim 0.175 \text{ meV} \sim 2 \text{ K},$$

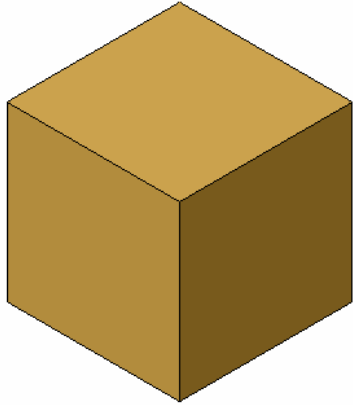
Considering the thermal broadening, it is necessary to have an ultra-low temperature STM (ULT-STM) workable at less than 1 K.

Wulff construction

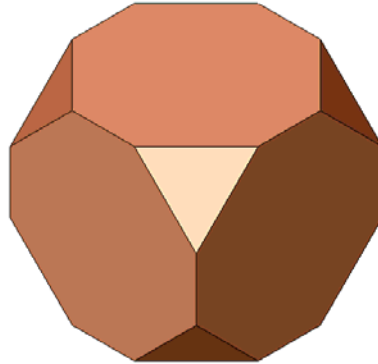


$$G = \int \gamma_s(\theta, \phi) dA$$

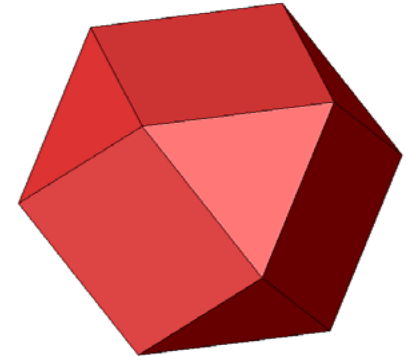
Single crystalline structures



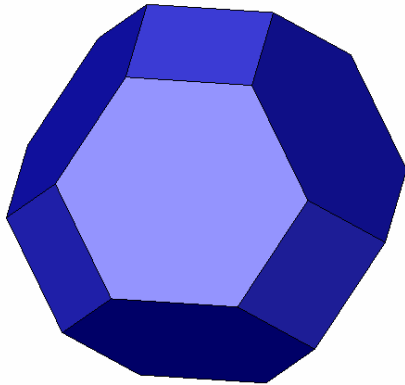
(a) cube



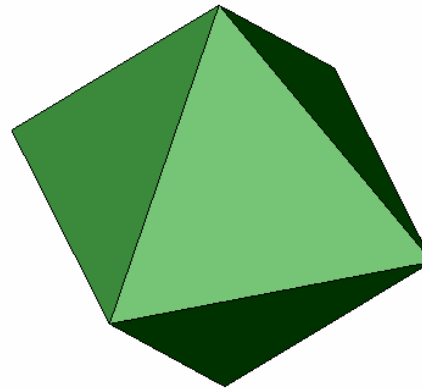
(b) truncated cube



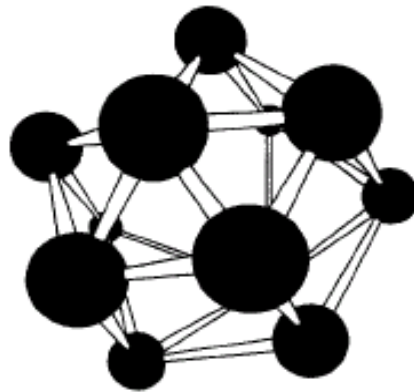
(c) cuboctahedron



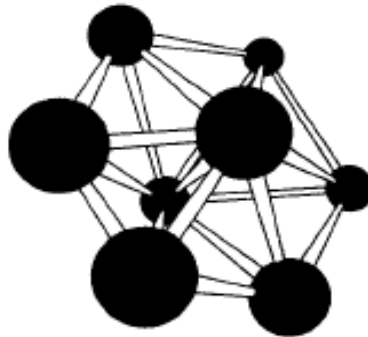
(d) truncated octahedron



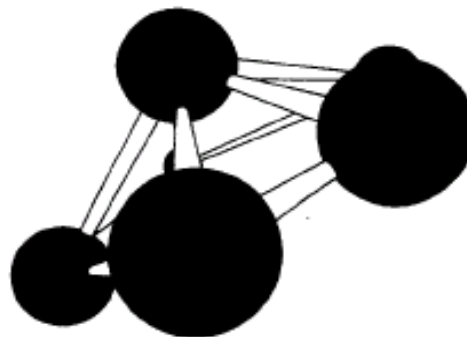
(e) octahedron



Icosahedra



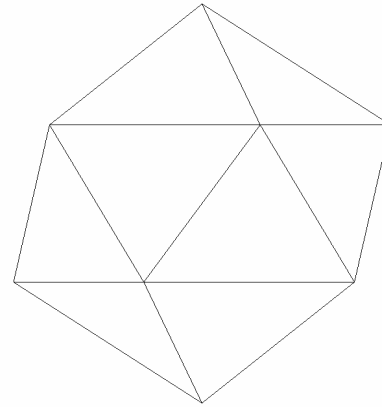
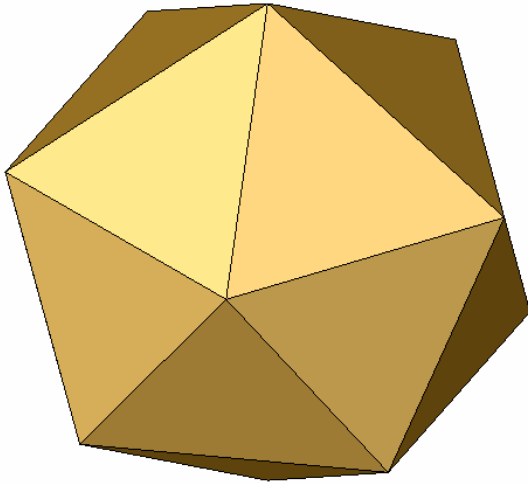
Decahedra



Pentagonal pyramid

Figure 4.8. Illustration of some calculated structures of small boron nanoparticles. (F. J. Owens, unpublished.)

Icosahedra

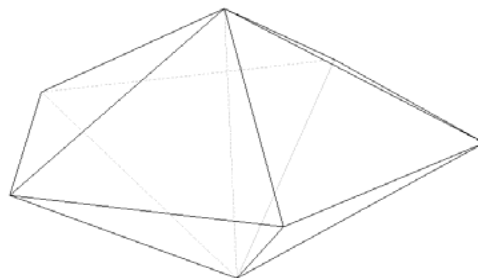
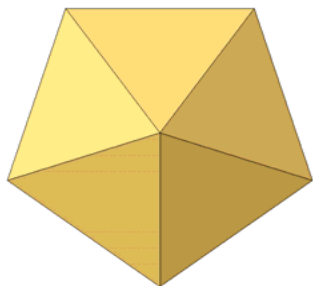


Size-dependent structures calculated for Ni clusters:
Icosahedra for 142 – 2300 atoms;
Marks' decahedra for 2300 – 17000 atoms;
Single crystal for > 17000 atoms.

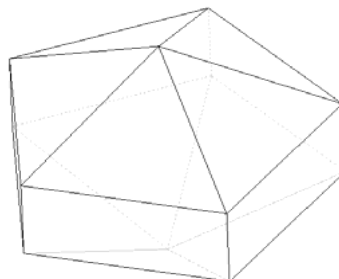
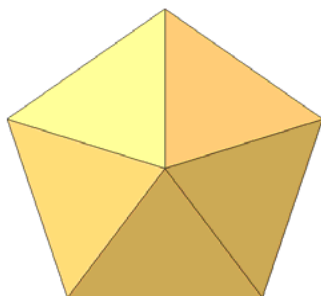
C.L. Cleveland and Uzi Landman, J. Chem. Phys. 94, 7376 (1991).



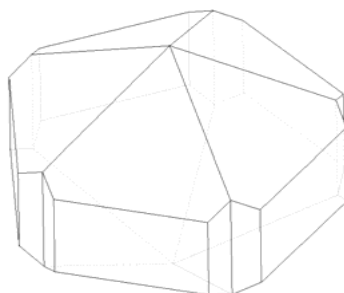
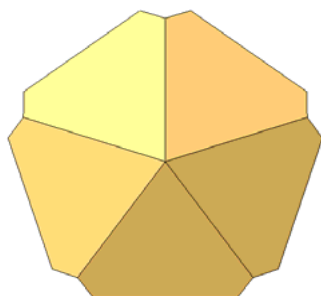
Decahedra



Classic



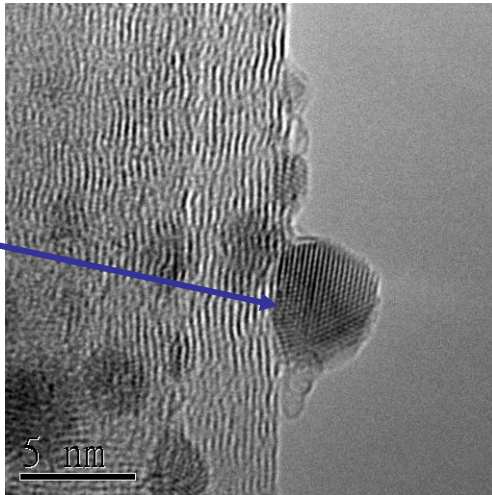
Ino's



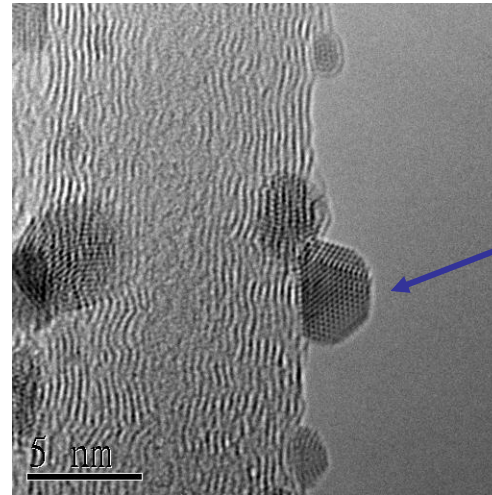
Marks'

Varying structures of Ag clusters

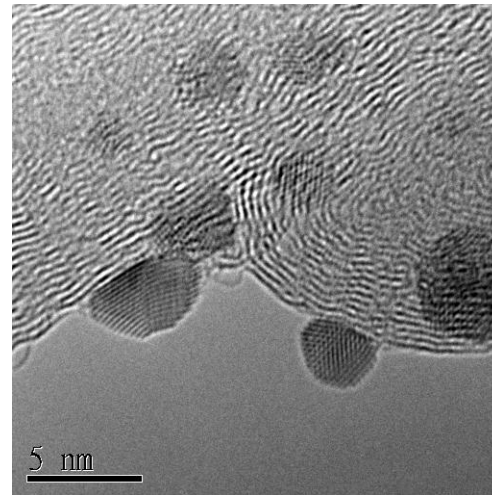
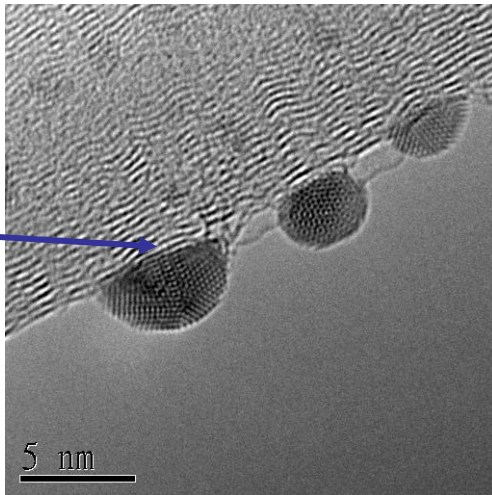
SC



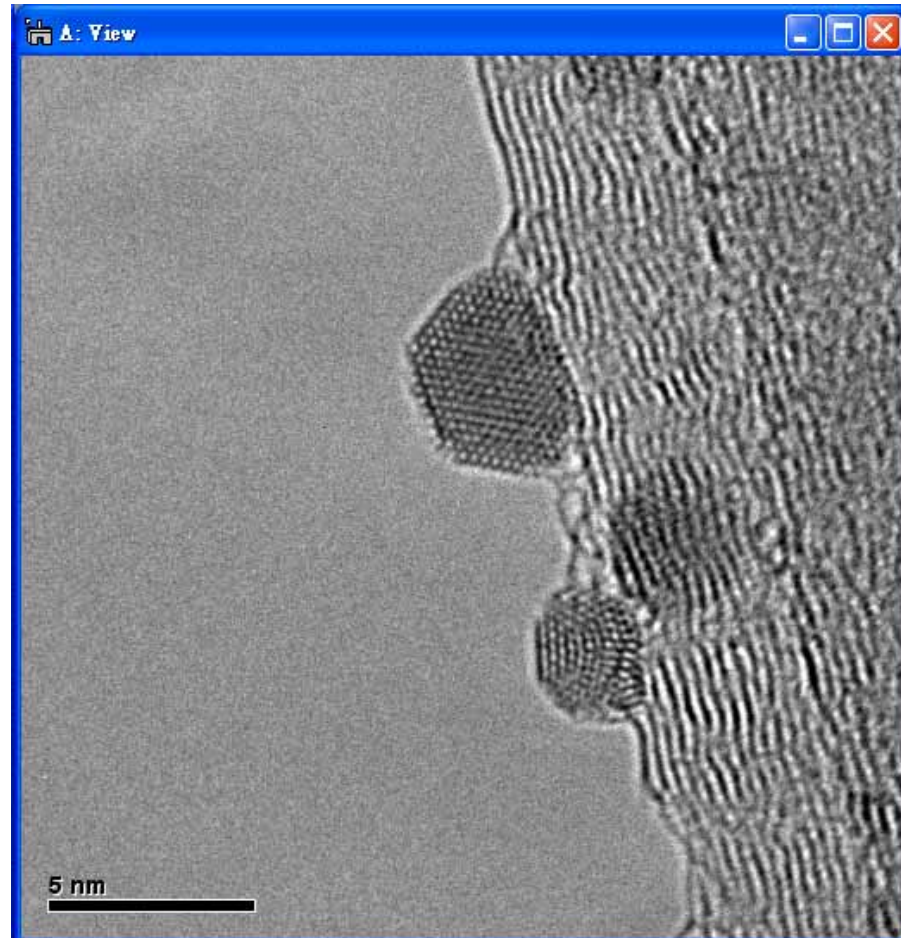
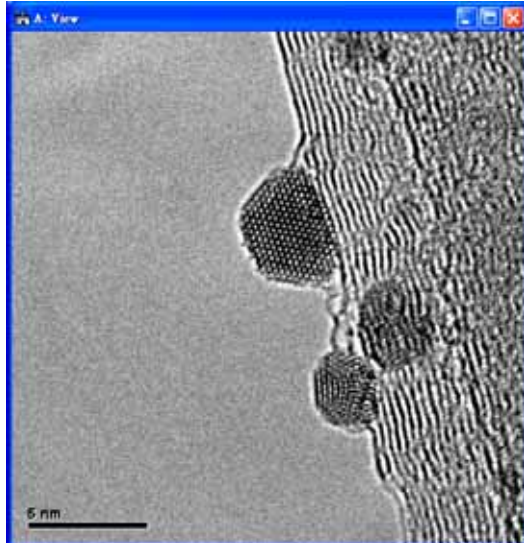
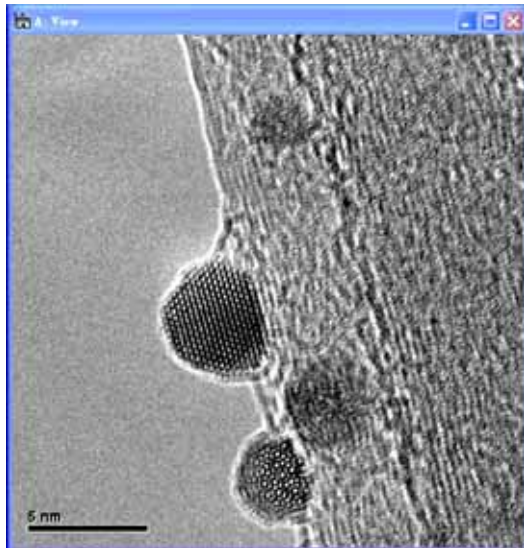
Dh



Ic

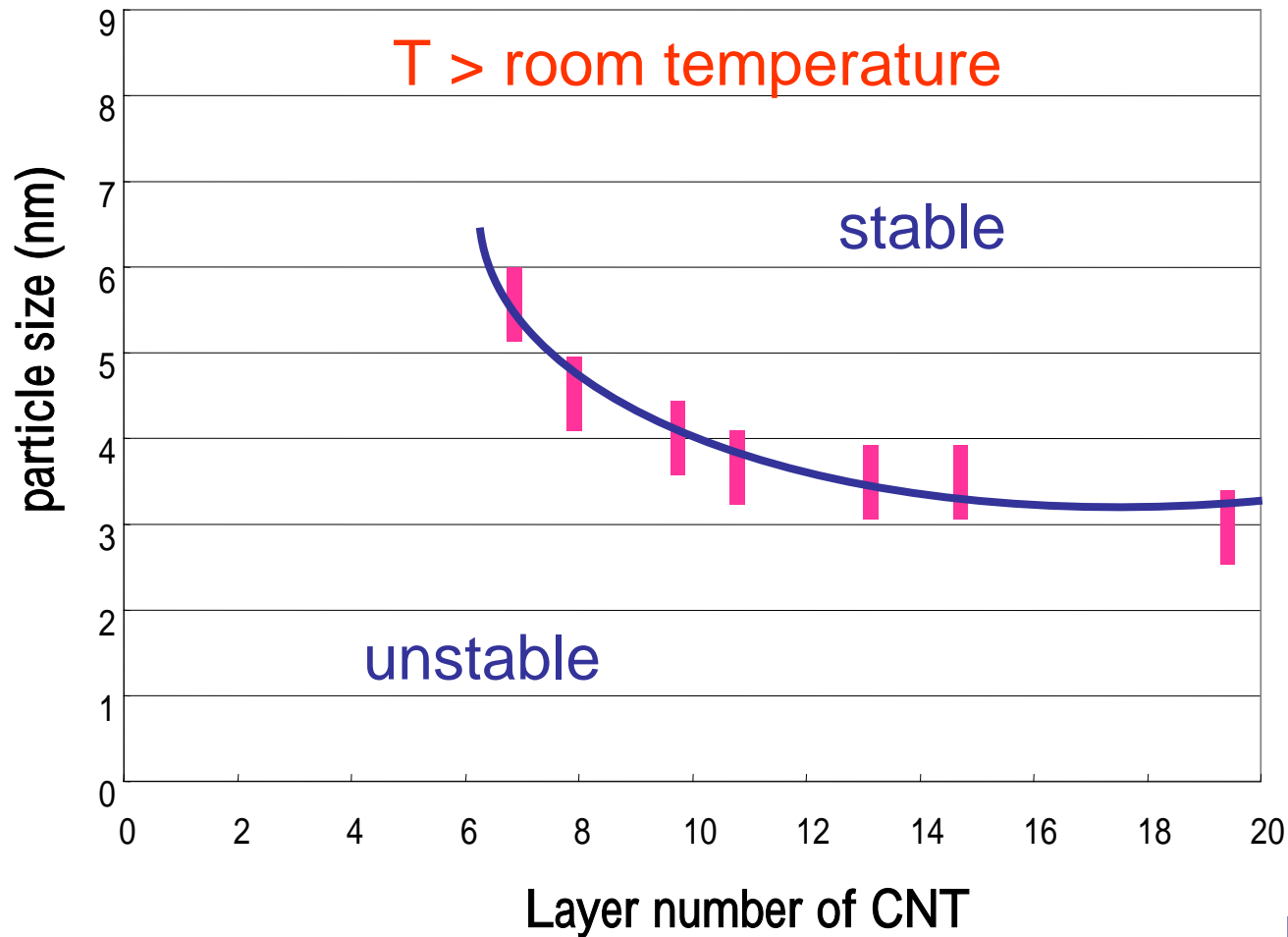


Atomic motion and recrystallization



Room temperature

Stability of crystalline phases



Magic clusters

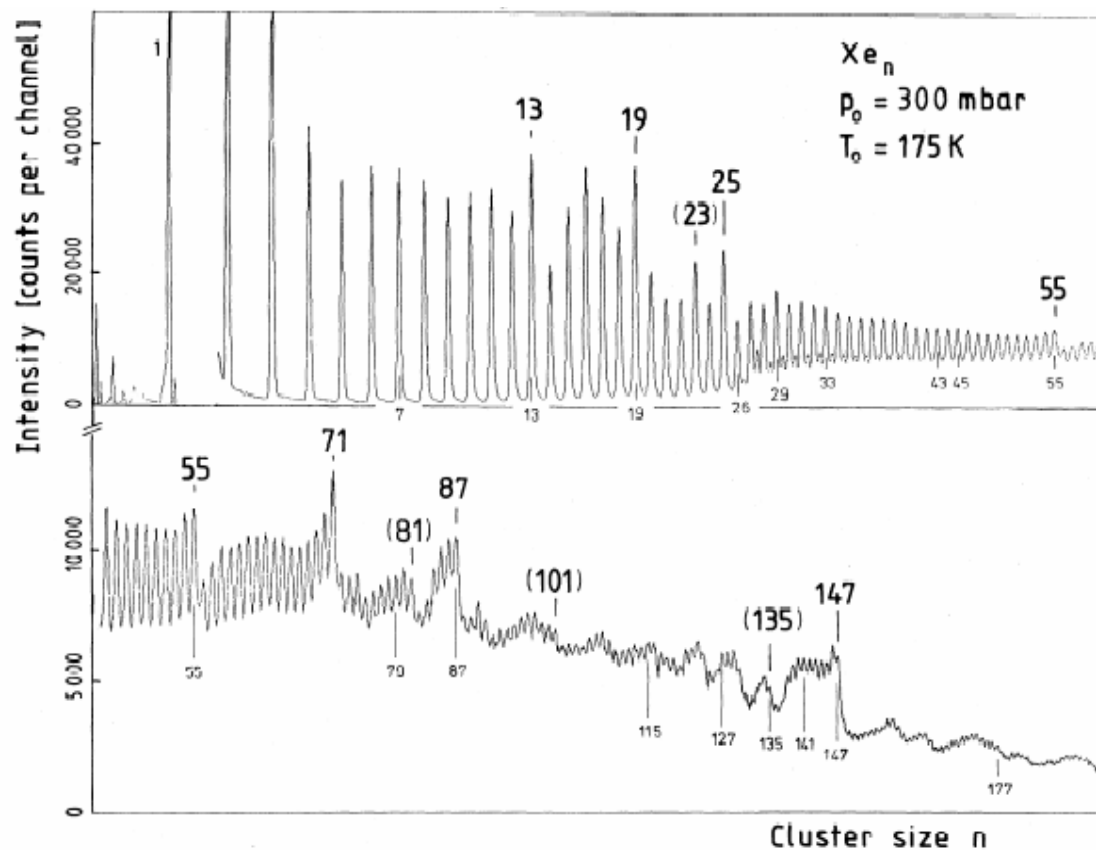
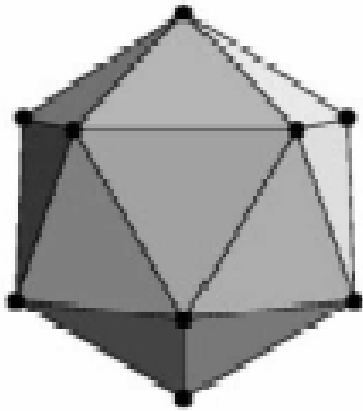


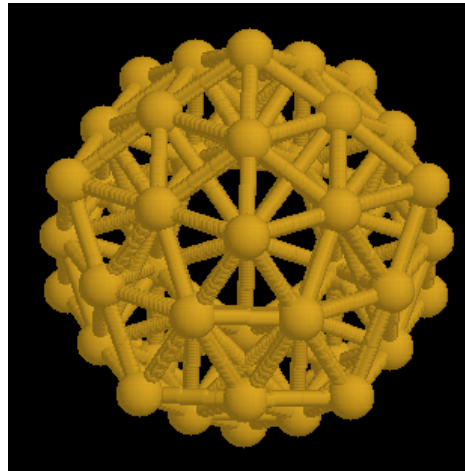
FIG. 1. Mass spectrum of xenon clusters. Observed magic numbers are marked in boldface; brackets are used for numbers with less pronounced effects. Numbers below the curve indicate predictions or distinguished sphere packings.

Mackay icosahedra

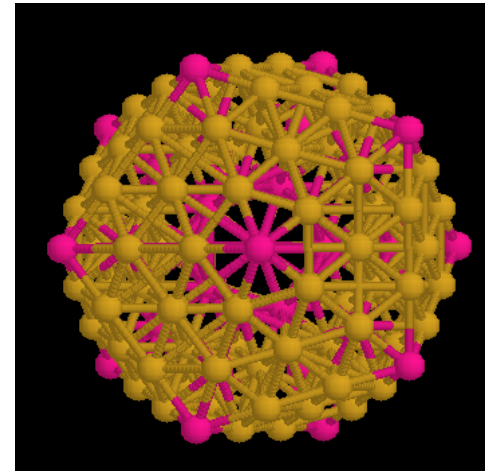


$P = 1$

20 fcc(111) faces



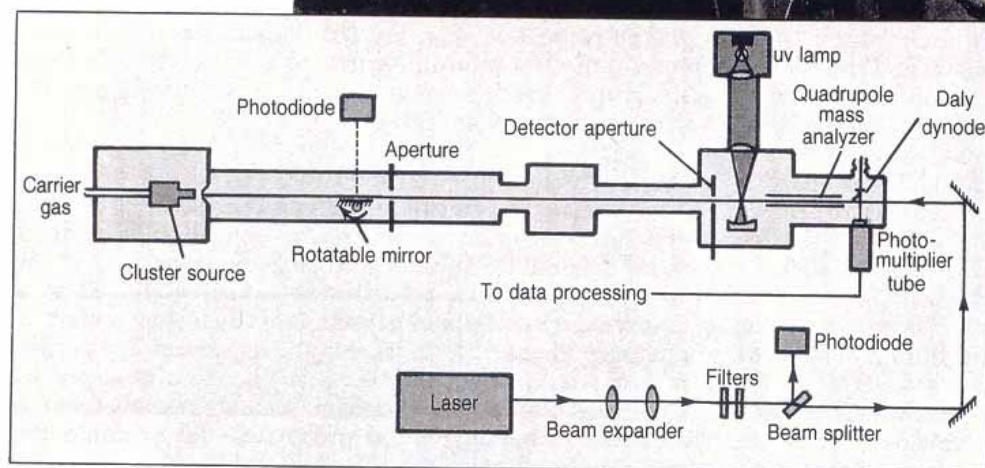
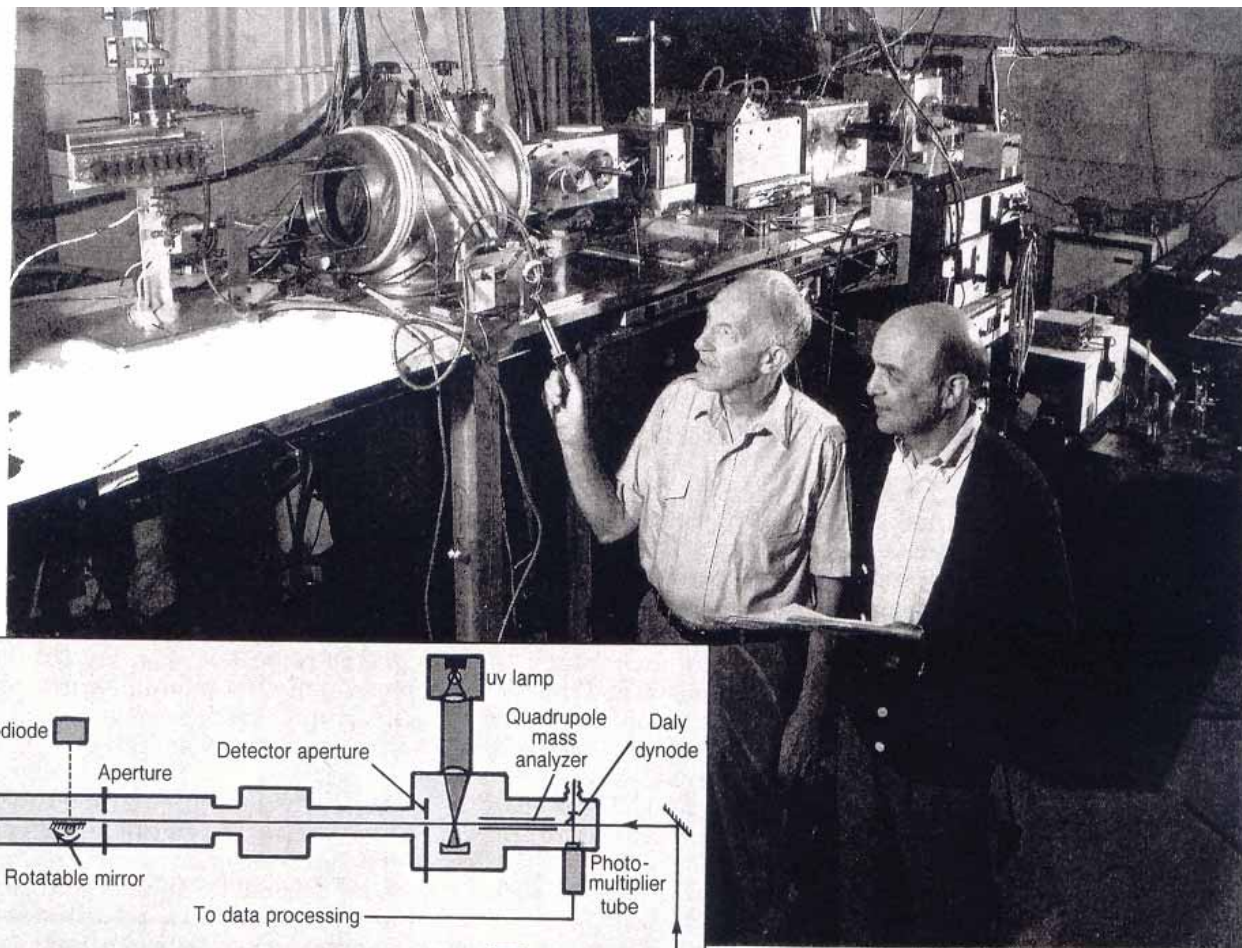
$P = 2$



$P = 3$

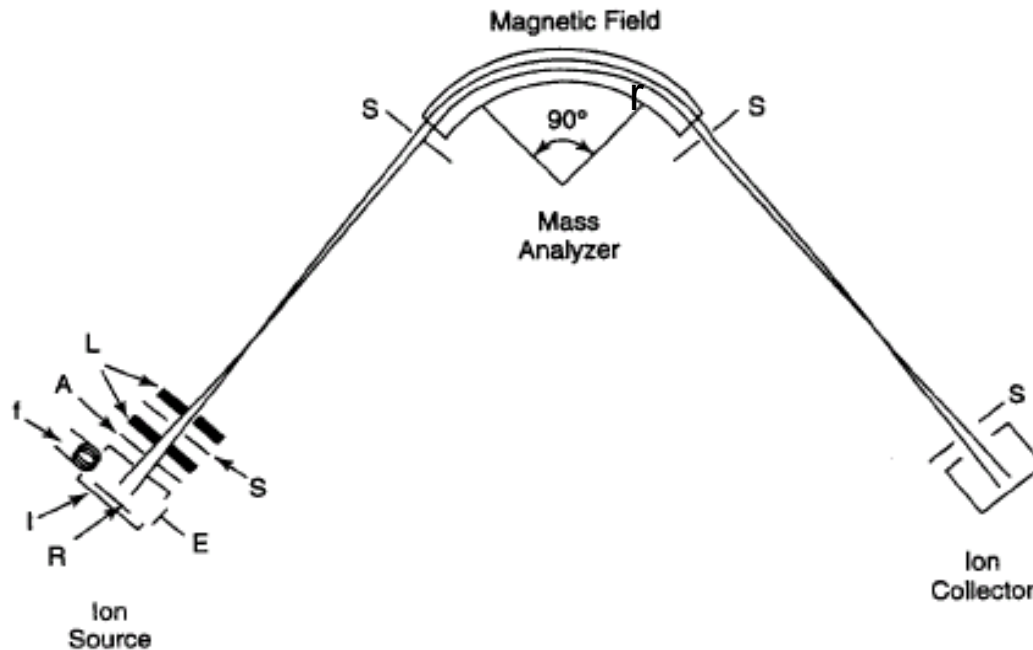
Shell model

$$N = 1 + \sum (10p^2 + 2)$$



Mass Analyzer

⊙ B



$$qV = \frac{1}{2} mv^2$$

$$F = qvB = mv^2/r$$

$$m/q = \frac{1}{2} B^2 r^2 / V$$

Figure 3.8. Sketch of a mass spectrometer utilizing a 90° magnetic field mass analyzer, showing details of the ion source: A—accelerator or extractor plate, E—electron trap, f—filament, I—ionization chamber, L—focusing lenses, R—repeller, S—slits. The magnetic field of the mass analyzer is perpendicular to the plane of the page.

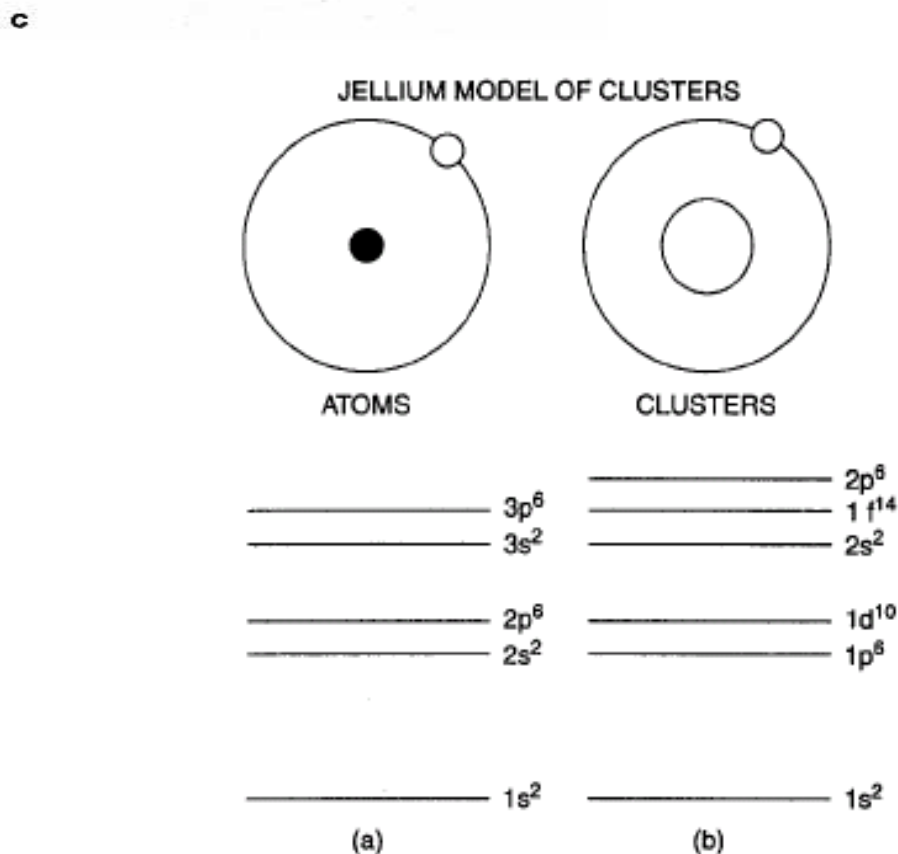
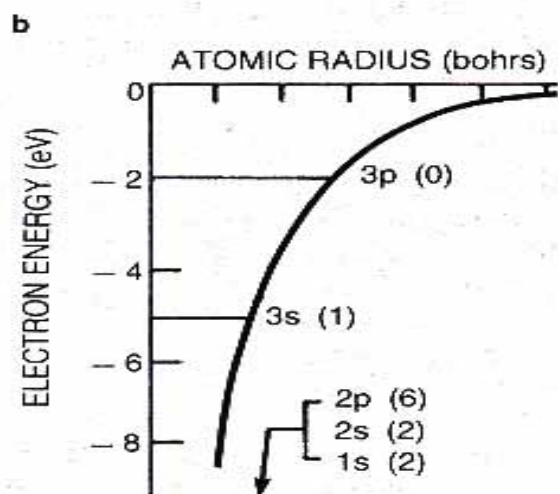
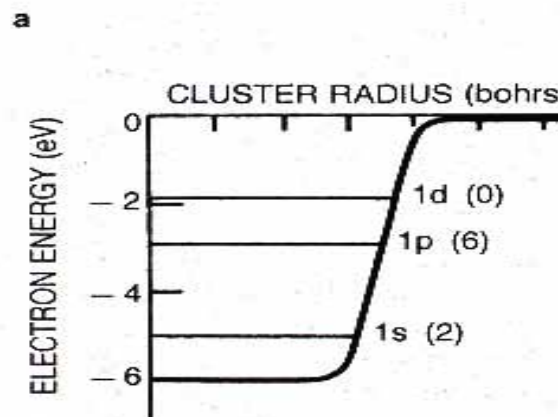
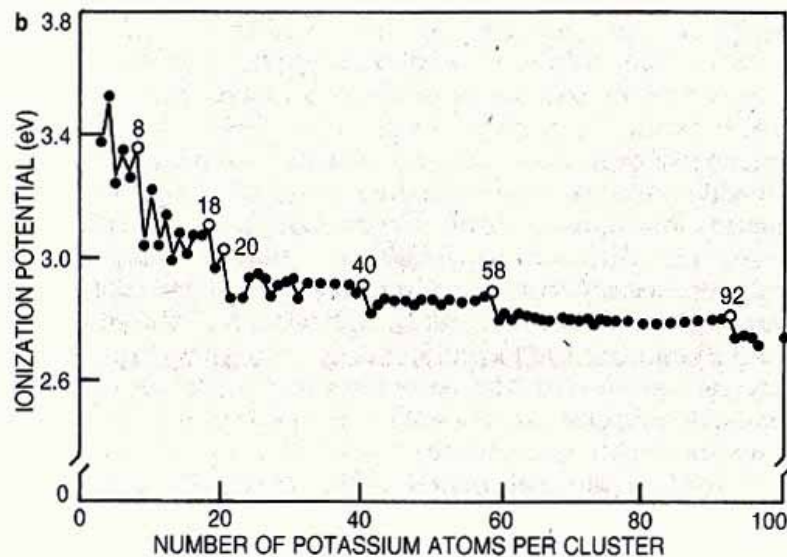
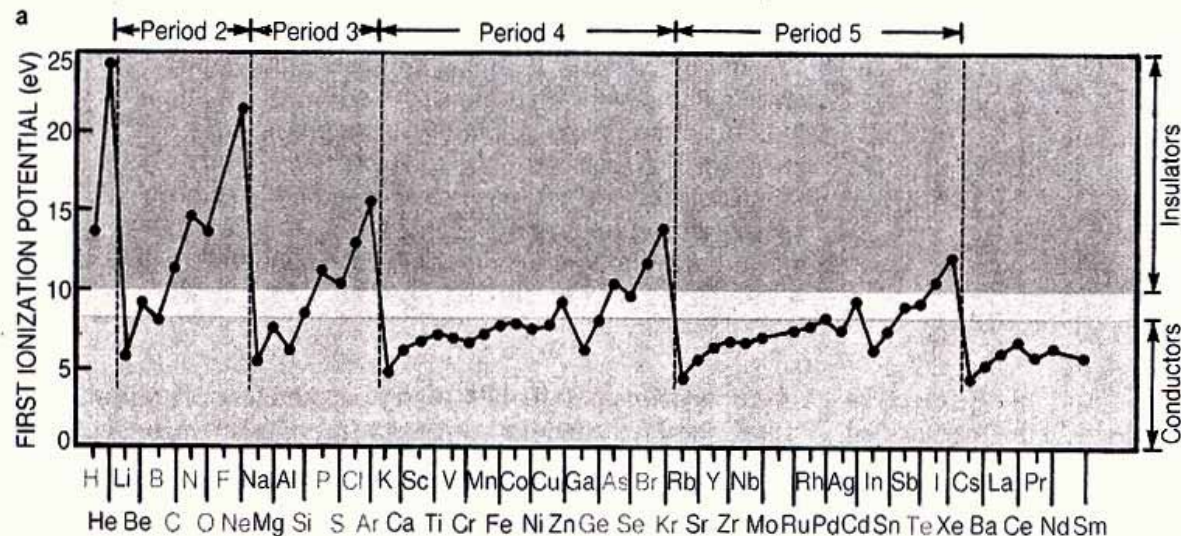
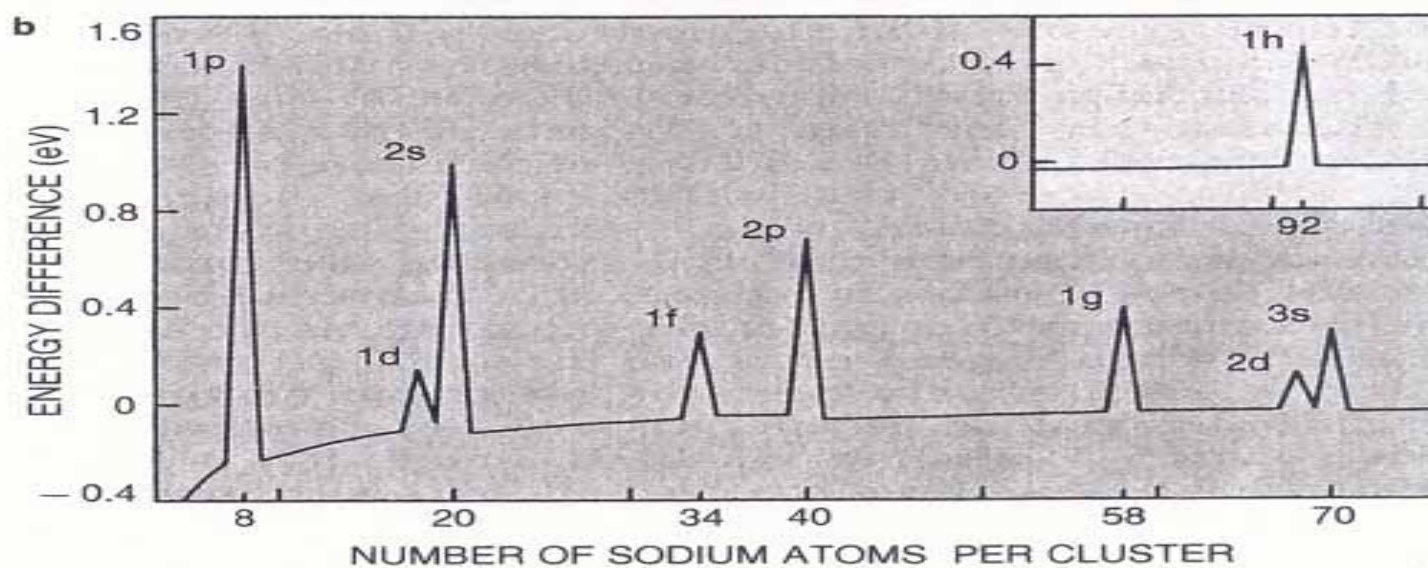
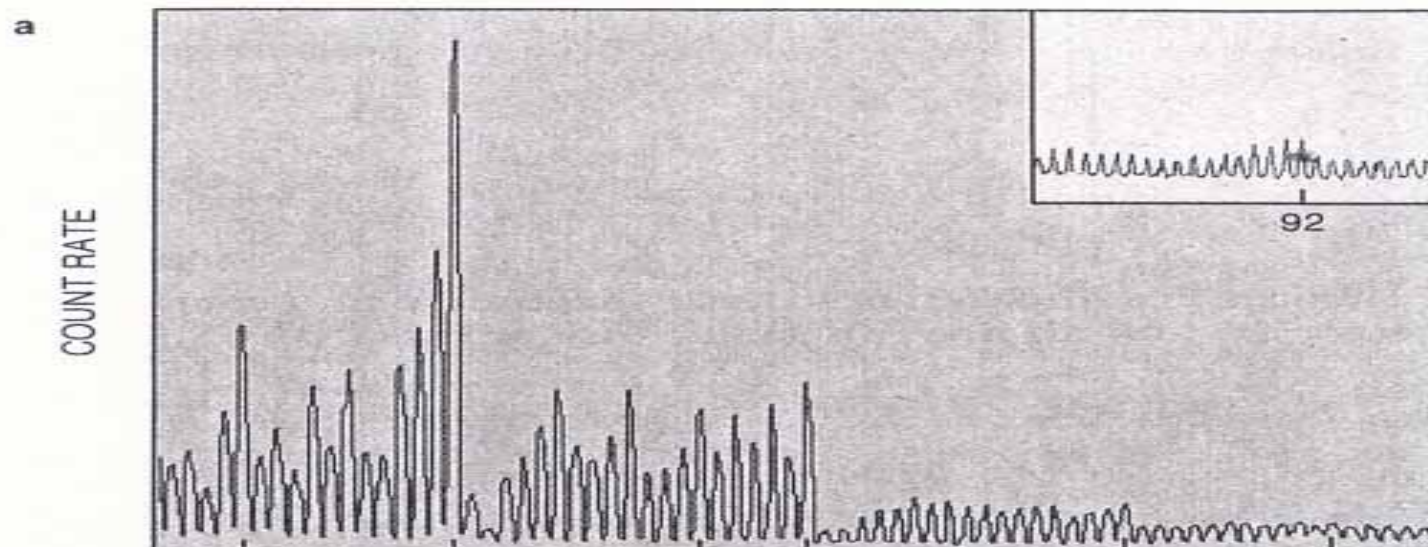
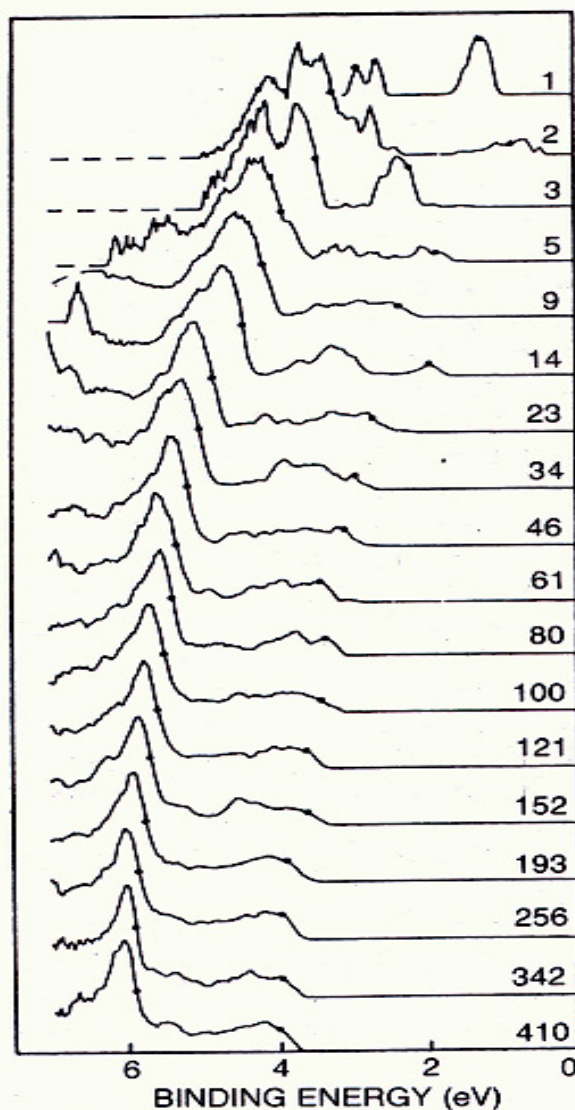


Figure 4.5. A comparison of the energy levels of the hydrogen atom and those of the jellium model of a cluster. The electronic magic numbers of the atoms are 2, 10, 18, and 36 for He, Ne, Ar, and Kr, respectively (the Kr energy levels are not shown on the figure) and 2, 18, and 40 for the clusters. [Adapted from B. K. Rao et al., *J. Cluster Sci.* **10**, 477 (1999).]



Shell structure: Two views. **a:** Atomic ionization potentials drop abruptly from above 10 eV following the shell closings for the noble gases (He, Ne, Ar and so on). For semiconductors (labeled in blue) the ionization potential is between 8 and 10 eV, while for conductors (red) it is less than 8 eV. It is clear that bulk properties follow from the natures of the corresponding atoms. (Adapted from A. Holden, *The Nature of Solids*, © Columbia U. P., New York, 1965. Reprinted by permission.) **b:** Ionization potentials for clusters of 3 to 100 potassium atoms show behavior analogous to that seen for atoms. The cluster ionization potential drops abruptly following spherical shell closings at $N = 8, 20, 40 \dots$. Features at $N = 26$ and 30 represent spheroidal subshell closings. The work function for bulk potassium metal is 2.4 eV. **Figure 3**





Ultraviolet photoemission spectra of ionized copper clusters Cu_N^- ranging in size from N of 1 to 410 show the energy distribution versus binding energy of photoemitted electrons. These photoemission patterns show the evolution of the 3d band of Cu as a function of cluster size. As the cluster size increases, the electron affinity approaches the value of the bulk metal work function. (Adapted from ref. 10.) **Figure 5**

Reactivity of nanoclusters

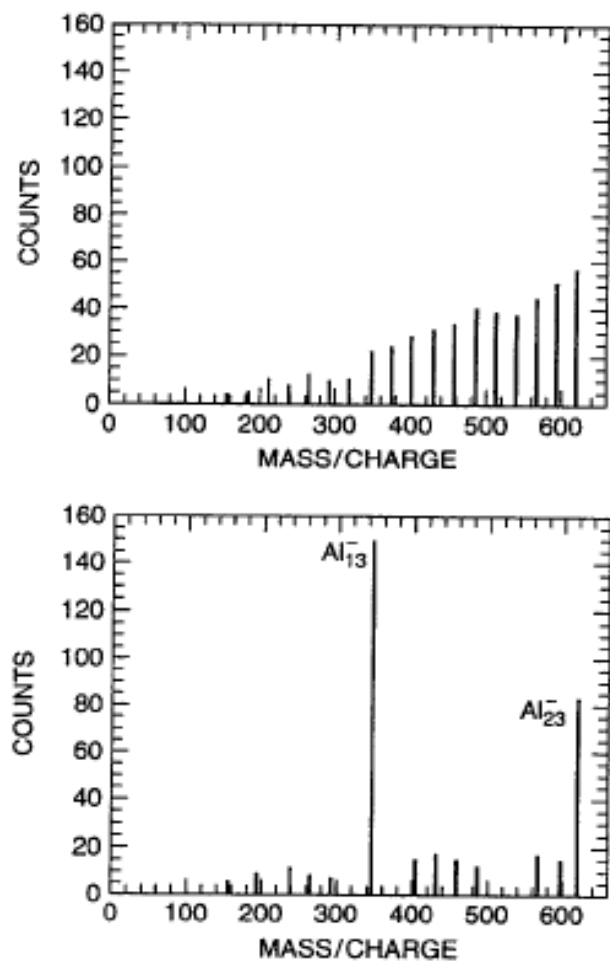
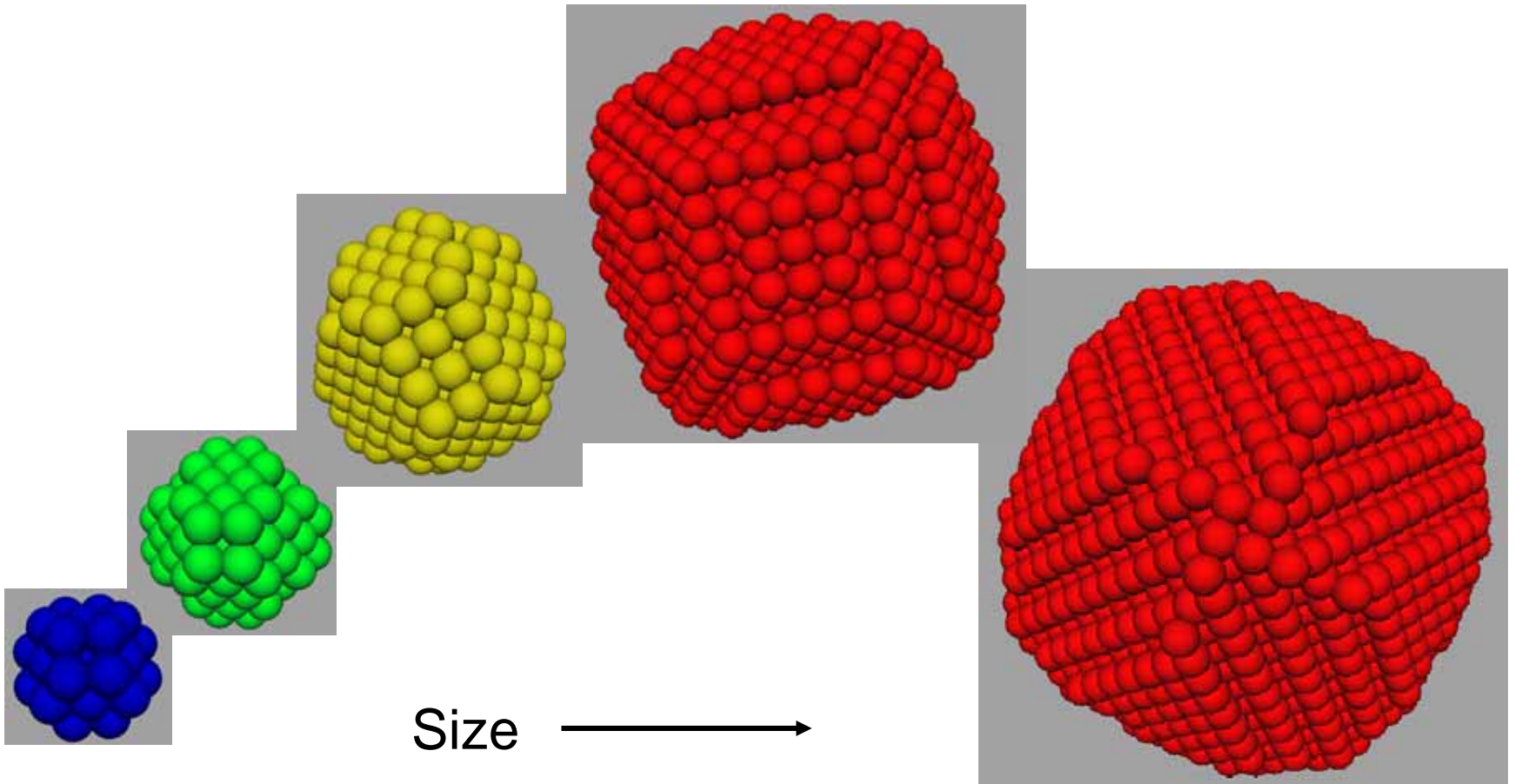
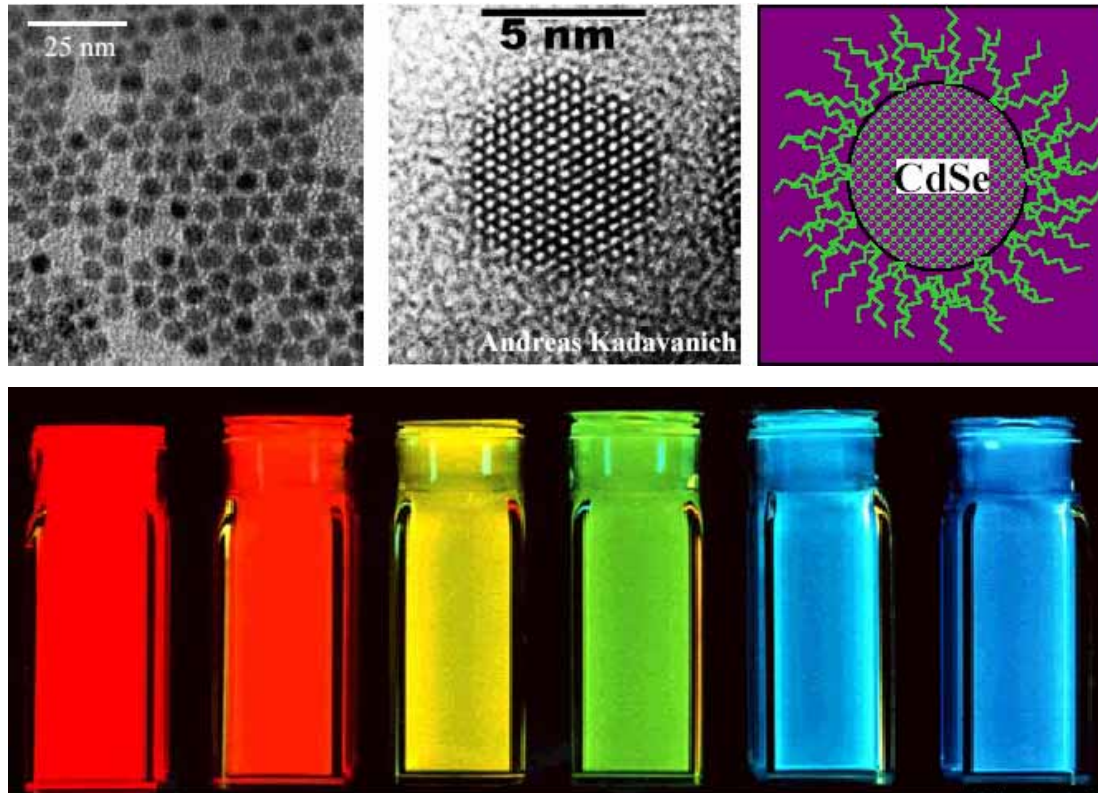


Figure 4.13. Mass spectrum of Al nanoparticles before (top) and after (bottom) exposure to oxygen gas. [Adapted from R. E. Leuchtner et al., *J. Chem. Phys.*, **91**, 2753 (1989).]

Size effect

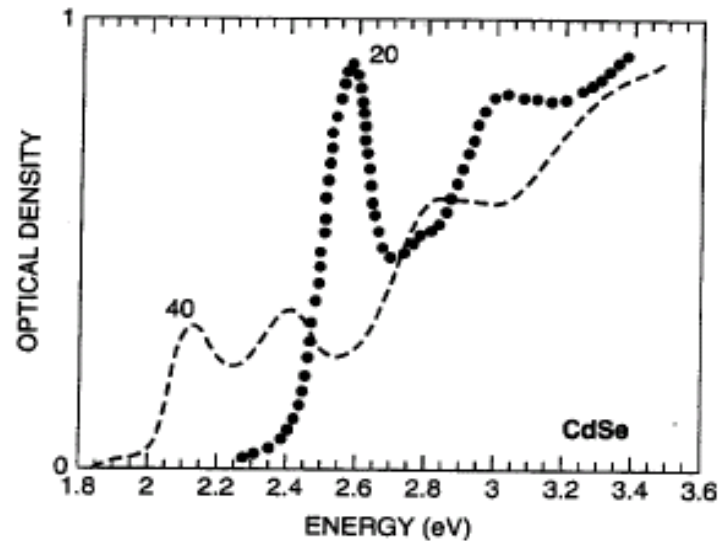
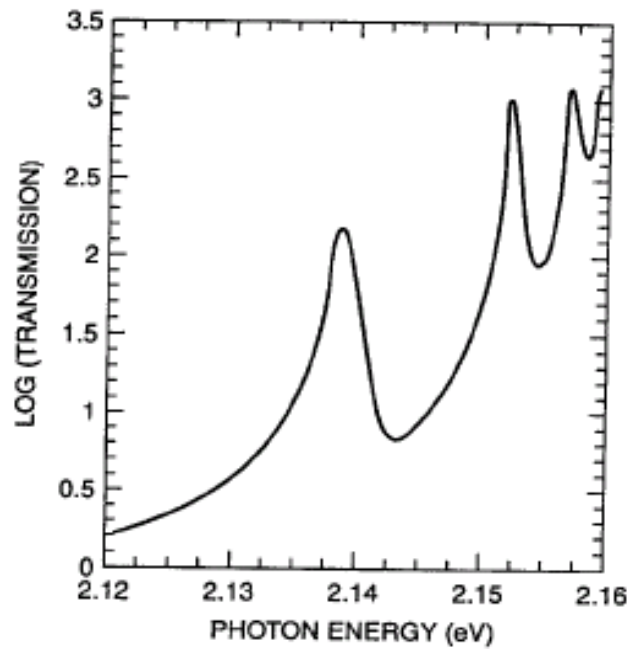


Semiconductor quantum dots



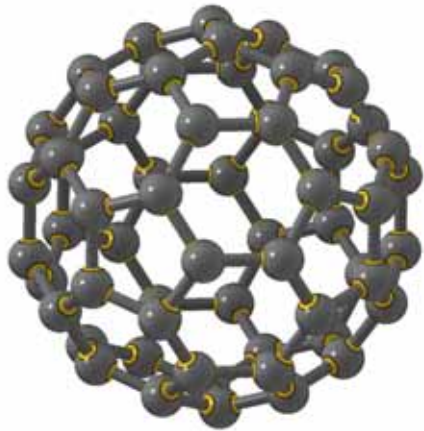
(Reproduced from Quantum Dot Co.)

Optical properties

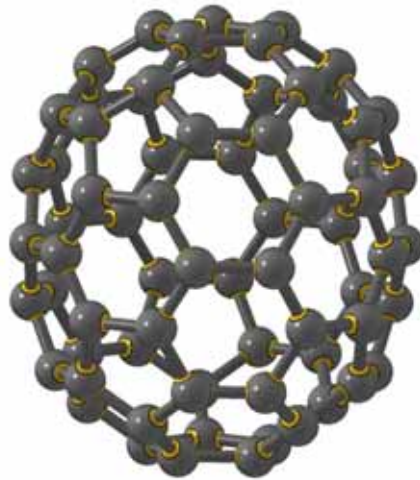


Optical absorption spectrum of CdSe for two nanoparticles having sizes 20 Å and 40 Å. [Adapted from D. M. Mittleman, *Phys. Rev. B* **49**, 14435 (1994).]

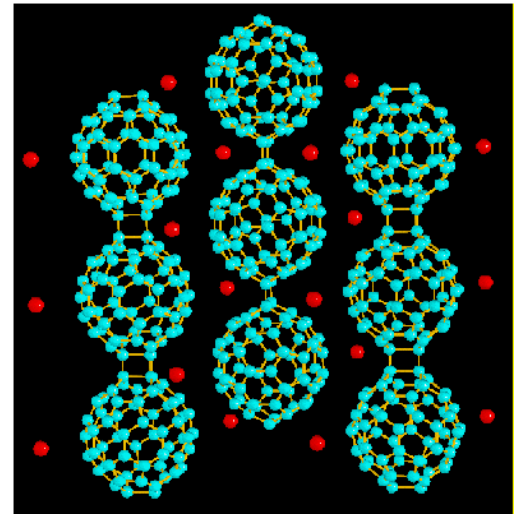
Fullerenes



C_{60}



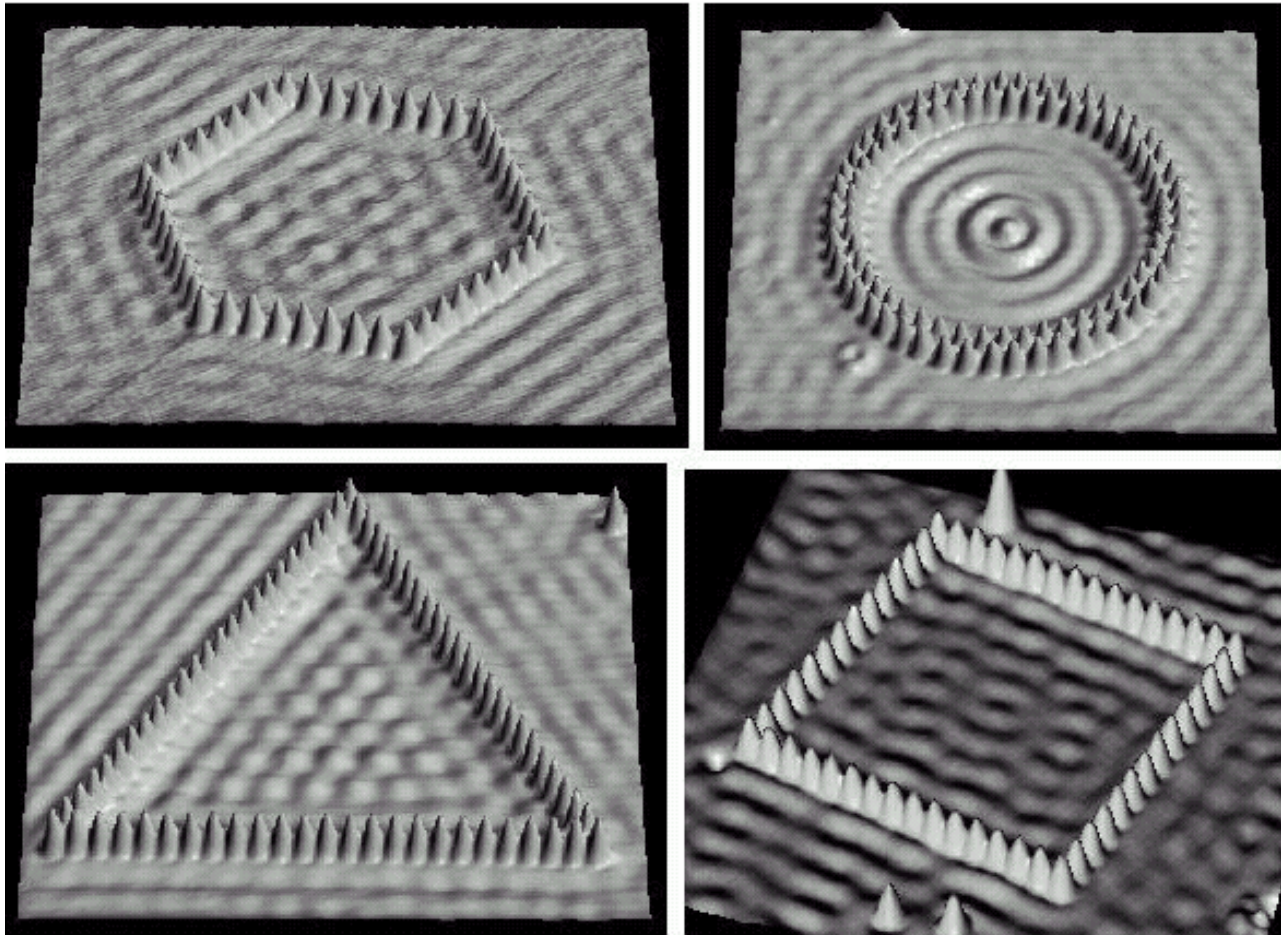
C_{70}



Rb_3C_{60}

$T_c = 29 \text{ K}$

Quantum corral



D.M. Eigler, IBM, Amaden

Artificial atom

